SUPPLEMENTARY FIGURES

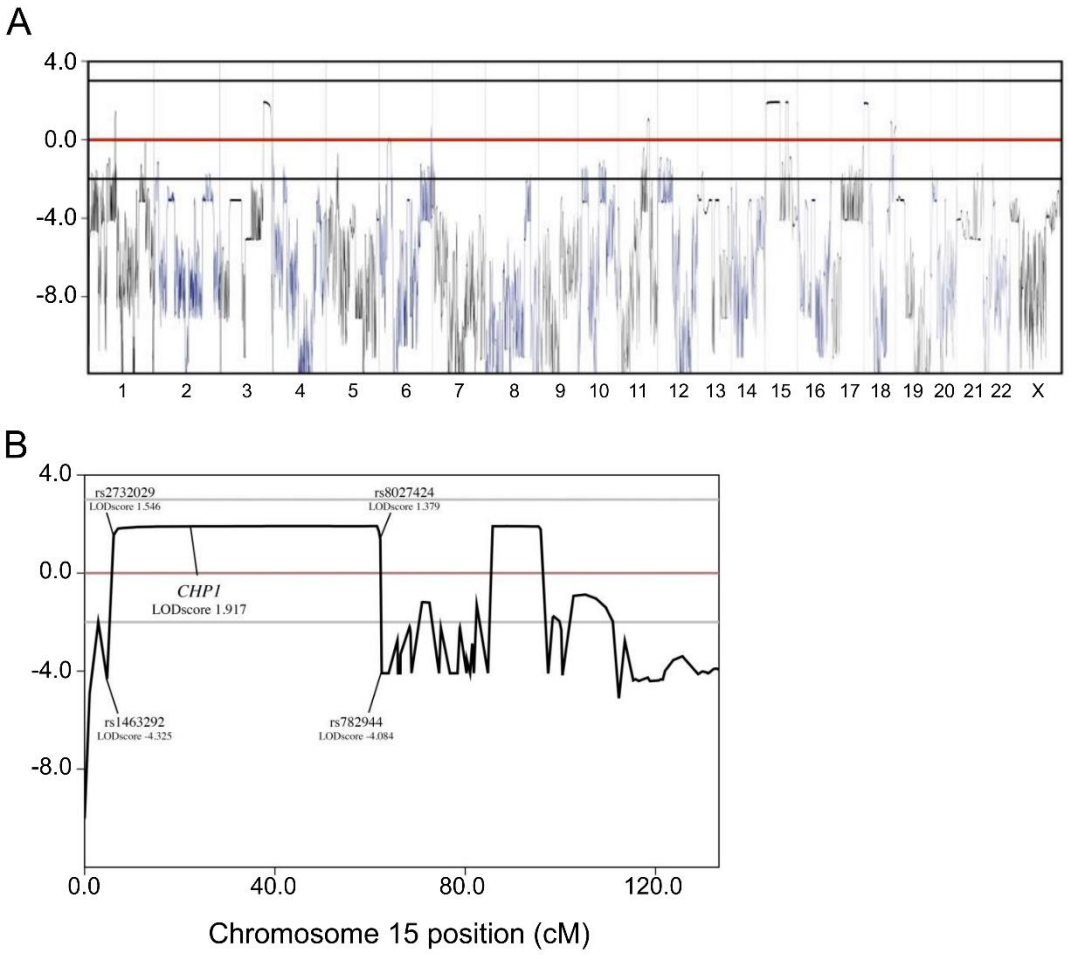

Supplementary Figure e-1. Multipoint linkage analysis

(A) Genotypes were available for five individuals, including affected subjects 6 and 8 and their relatives, 1, 2 and 7. An autosomal recessive transmission under 0.90 penetrance model with equal allele frequencies, similar recombination fractions between males and females, and a disease frequency of 0.00001 were assumed. WGLA did not lead to the identification of a unique well-defined associated locus due to pedigree structure and size limitations. Various putatively linked or unexcluded (LOD scores above -2) loci were found in the family. **(B)** WGLA detail in chromosome 15 region. LODscores and coordinates for linked regions are depicted.

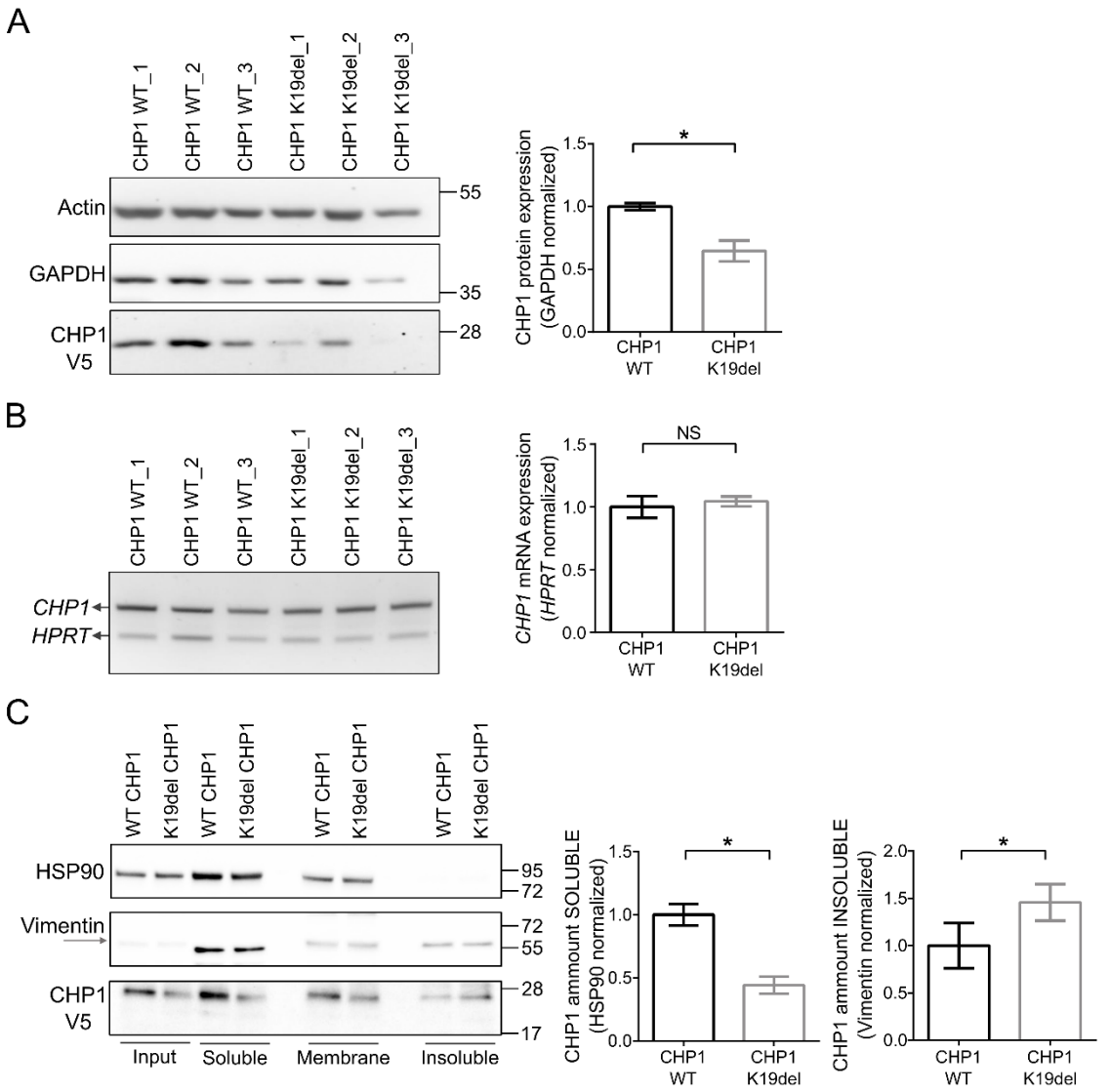

Supplementary Figure e-2. K19del mutation affects the expression and solubility of CHP1 in N2A cells

(A) WB from HEK293T lysates transiently expressing CHP1-WT-V5, CHP1-K19del-V5 or empty V5-vector (control) collected 48h upon transfection. Protein lysates were probed with antibodies against V5, to detect CHP1 WT and mutant proteins, and GAPDH as loading control. Graph represents quantification of CHP1 relative expression. Bars show the mean ± SEM. * denotes statistically significance ($p \leq 0.05$ two-tailed Student's t-test) between CHP1-WT and CHP1-K19del expression. **(B)** Determination of *CHP1-WT-V5* and *K19del-V5* transcripts by semi-quantitative RT-PCR. RNA samples were collected 48h upon transfection. Graph represents quantification of *CHP1-V5* transcripts normalized to *HPRT* expression. Bars show the mean ± SEM. NS denotes no significant difference ($p > 0.05$ two-tailed Student's t-test) between CHP1-WT and CHP1-K19del transcripts. **(C)** Subcellular fractionation of protein lysates from N2A transiently overexpressing CHP1-WT-V5 or CHP1-K19del-V5. Lysates were separated into soluble (cytoplasmic) and insoluble (cytoskeletal) fractions by differential lysis and centrifugation. Representative WB from total lysates and fractions were stained with V5 antibodies for WT and mutant CHP1. HSP90 and vimentin were used as enrichment markers for soluble and insoluble fractions, respectively. A strong unspecific band was detected only in the cytoplasmic fraction upon vimentin antibody probing. Arrow indicates the specific

vimentin band (upper and faint). Graphs represents quantification of relative expression of CHP1 in the soluble and insoluble fractions. Bars show the mean ± SEM from 3 independent blots. * denotes statistically significance ($p \leq 0.05$ two-tailed Student's t-test) between CHP1-WT and CHP1-K19del expression.

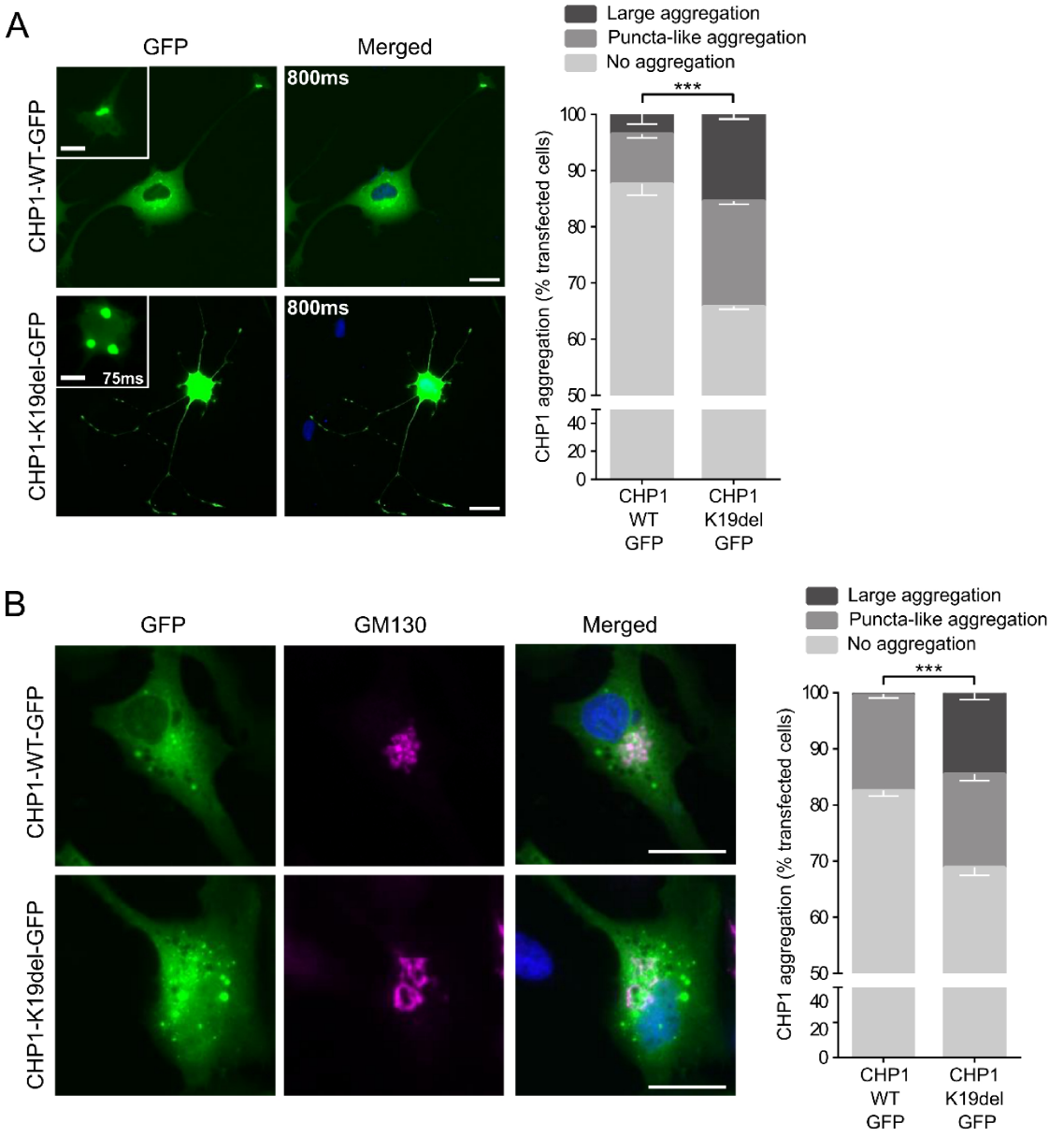

Supplementary Figure e-3. Massive protein aggregation in HeLa and PC12 cells expressing mutant CHP1

(A) Representative images of differentiated PC12 cells transiently expressing WT and mutant CHP1-GFP. CHP1-WT-GFP is expressed both in the cell body and neurite-like structures of PC12 cells. Small puncta-like aggregates in axon projection is magnified in the inset. CHP1-K19del-GFP expression leads to large protein aggregation in the cell body. Inset depicts aggregate magnification with reduced exposure time. Green fluorescence exposure time is indicated in ms inside the panels. Scale bar of main images: 20µm and scale bar of magnification insets: 10µm. Graph represent aggregation quantification in GFP-positive cells. Bars show the mean ± SEM (error bars) from 3 independent experiments (n ≥ 130). *** denotes statistically significance ($p<0.001$ Chi-square test). **(B)** Representative images of HeLa cells transiently expressing WT or mutant CHP1-GFP. Few puncta-like aggregates and protein perinuclear expression can be observed in cells expressing CHP1-WT-GFP. Expression of CHP1-K19del-GFP leads to formation of large protein aggregates distributed throughout the cell. Perinuclear expression of mutant CHP1 is also evident. Immunostaining with the *cis* Golgi marker

G130, in magenta, colocalise with CHP1 proteins expression in merged image. Scale bar: 20µm. Graph represents aggregation quantification in GFP-positive cells. Bars show mean ± SEM (error bars) from 3 independent experiments ($n \geq 300$). *** denotes statistically significance ($p<0.001$ Chi-square test).

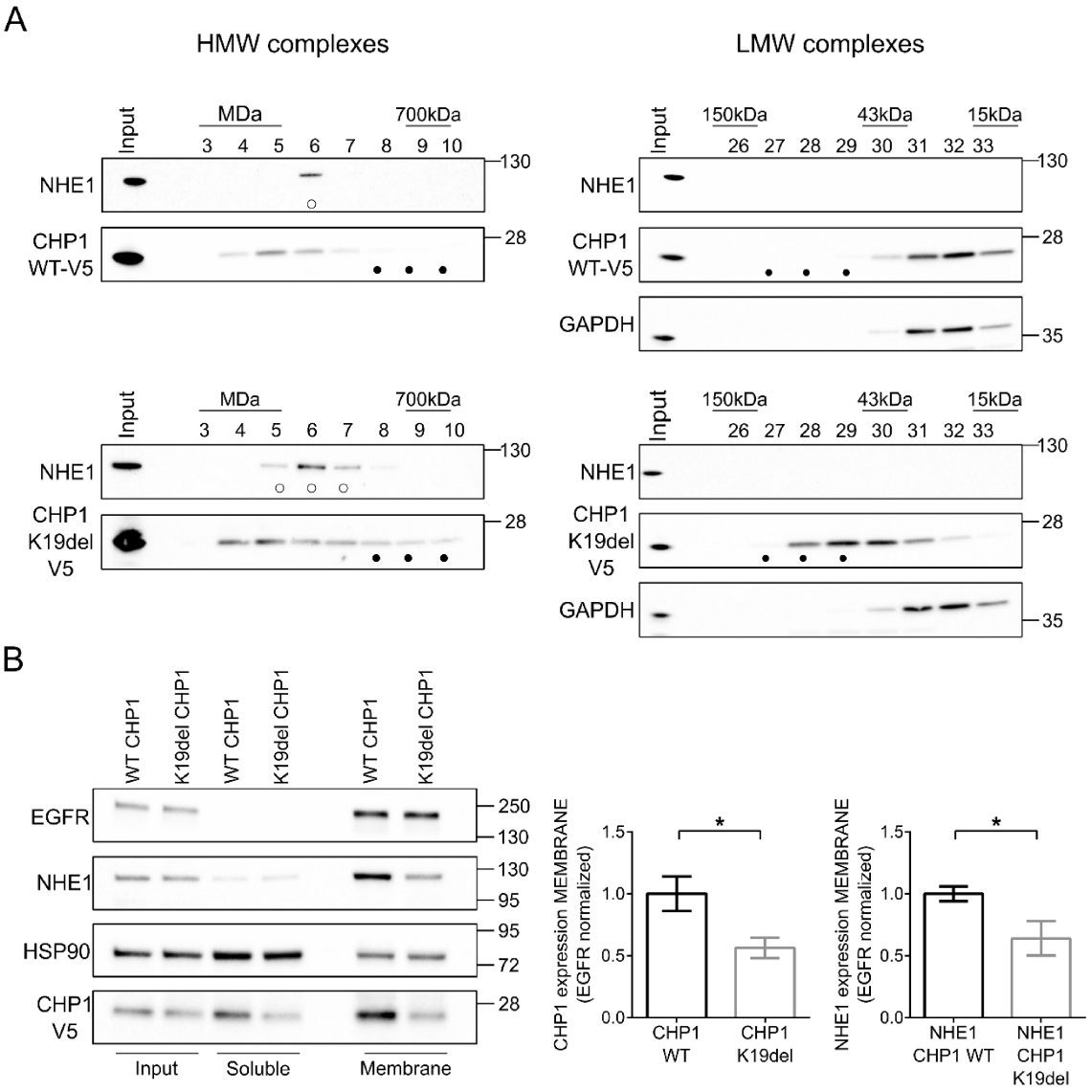

Supplementary Figure e-4: The K19del mutation alters NHE1 elution in HMW complexes and impairs NHE1 membrane targeting in N2A cells

(A) Size exclusion chromatography of protein extracts from HEK293T cells expressing WT and mutant CHP1-V5. Representative fractions analysed by WB showing high molecular weight (HMW) and low molecular weight (LMW) complexes. Depicted molecular weights were calculated upon calibration and standard curve representation (not shown). Blots were probed with antibodies against V5, glycosylated NHE1 and GAPDH. Open circles denote differential NHE1 elution and bold circles denote CHP1 differential elution between WT and K19del protein lysates. **(B)** Subcellular fractionation of protein lysates from N2A transiently overexpressing CHP1-WT-V5 and CHP1-K19del-V5 proteins. Fractions were separated into soluble (cytoplasmic) and membrane fractions by differential lysis and centrifugation. Representative WB of total lysates and fractions stained with V5 antibodies for WT and mutant CHP1 and glycosylated NHE1. HSP90 and EGFR were used as enrichment markers for soluble and membrane fractions, respectively. Graphs represent quantification of relative expression of CHP1 and NHE1 in the membrane fraction. Bars show the mean ± SEM from 3 independent blots. * denotes statistically significance ($p \leq 0.05$ two-tailed Student's t-test)

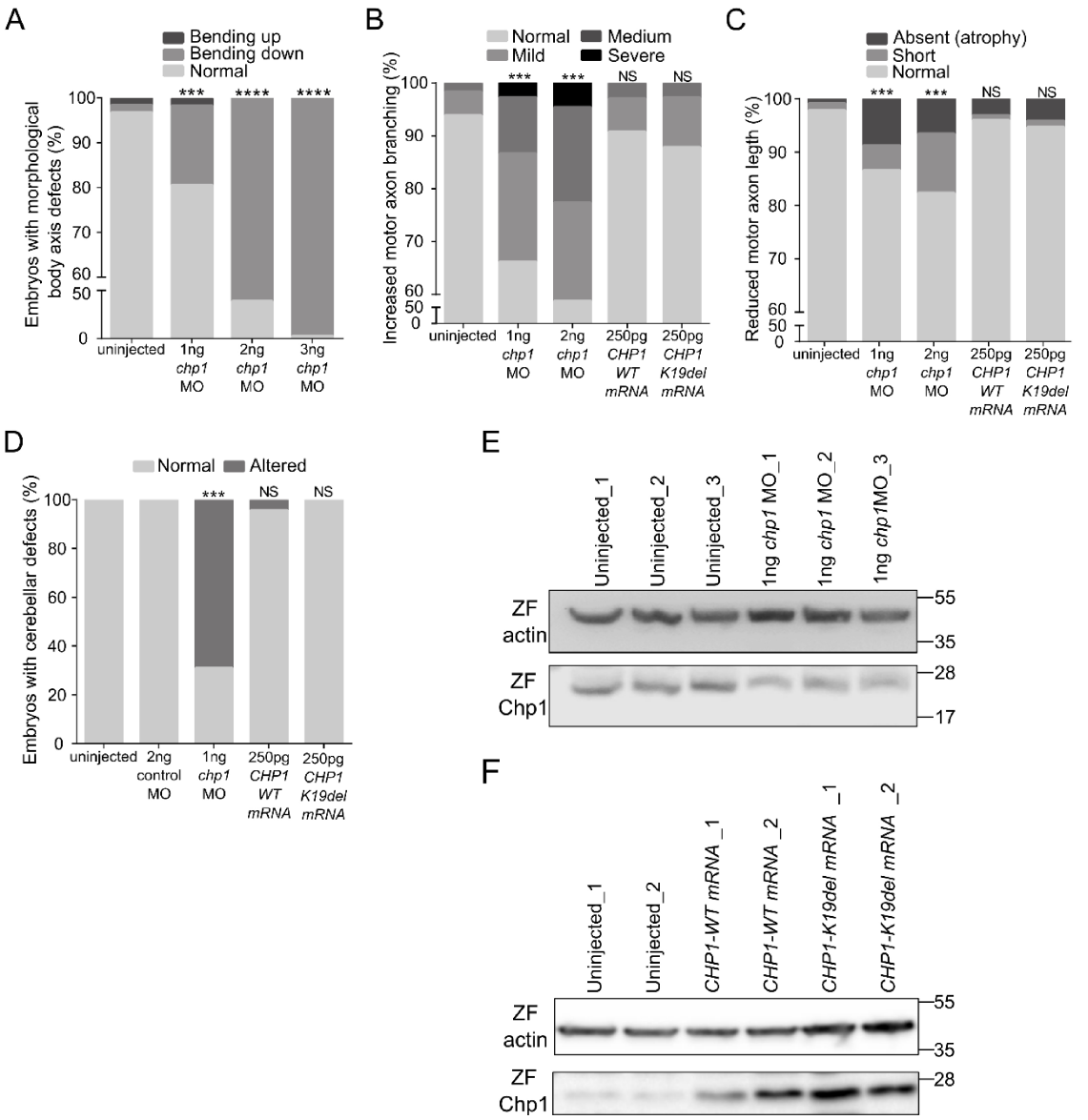

Supplementary Figure e-5. *chp1* MO dosage optimization and quantification of CaP-MN and cerebellar defects in control groups

(A) Quantitative analysis of body axis phenotype upon injection of increasing *chp1* MO concentrations. Embryos with axis defects were grouped in 3 categories: Bending up, bending down, and normal axis. Injection of 2 and 3ng of MO resulted in severe body axis bending upwards. Results are presented in percentages from n ≥ 60 observed zebrafish morphants representing 3 independent experiments. *** and **** denote statistically significance (p<0.001 and p<0,0001 Fischer exact test). **(B)** and **(C)** Quantitative analysis of CaP-MN demonstrates that two different *chp1* MO concentrations lead, in a dose-dependent manner, to abnormal CaP-MN terminal branching and increased axonal truncations. Injection of 250pg of human *CHP1-WT* or *K19del* human mRNAs cause negligible CaP-MN defects, in comparison to uninjected zebrafish. Results are presented in percentages from n ≥ 150 analysed axons representing 3 independent experiments. * and *** denote statistically significance (p≤0.05 and p<0.001 Fischer exact test). **(D)** Quantitative analysis of cerebellar defects indicates that injection of 2ng of control MO or 250pg of human *CHP1-WT* or *K19del* human mRNAs do not affect cerebellar morphology. Results are presented in

percentages from n ≥ 40 observed zebrafish morphants representing 3 independent experiments. * and *** denote statistically significance ($p \leq 0.05$ and $p < 0.001$ Fischer exact test). **(E)** WB analysis of uninjected and 1 ng *chp1* MO-injected zebrafish embryos (at ~34hpf) demonstrates knockdown efficiency. Blots were probed with antibodies against zebrafish Chp1 and β-actin (loading control). **(F)** WB of uninjected, and human WT and mutant *CHP1* mRNAs-injected zebrafish embryos (at ~34hpf) demonstrates efficient protein overexpression. Blots were probed with antibodies against human/zebrafish CHP1 and β-actin.

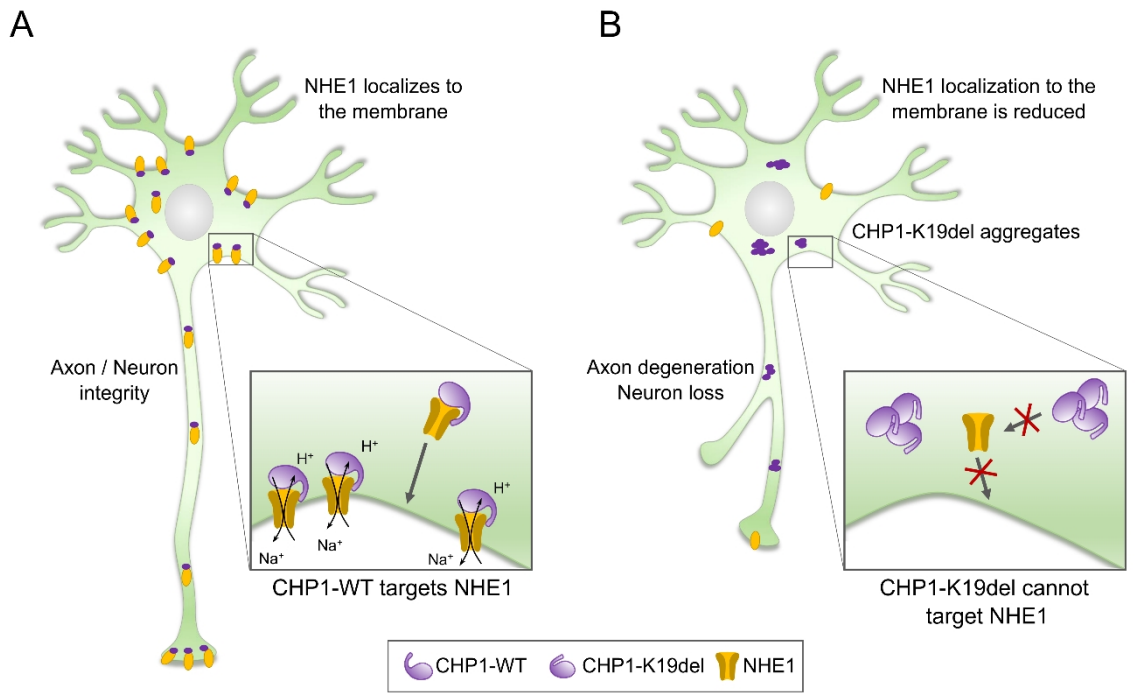

Supplementary Figure e-6. CHP1-mediated NHE1 dysregulation causes ataxia.

Diagrammatic representation of the molecular pathogenic mechanism for the CHP1-K19del mutation. **(A)** NHE1 is properly targeted to the membrane by CHP1, thus maintaining axonal pHi homeostasis and preserving axonal integrity. **(B)** Mutant CHP1 protein is misfolded and aggregates. Diminished CHP1 levels are insufficient to target NHE1 to the cellular membrane. NHE1 deficiency in axonal membranes alters pHi homeostasis thus leading to axonal degeneration and loss.